Cocontinuous Phase Morphology of Asymmetric Compositions of Polypropylene/High-density Polyethylene Blend by the Addition of Clay

Anup K. Dhibar,[1] Jin Kon Kim,[2] Bhanu B. Khatua[1]

[1]*Materials Science Centre, Indian Institute of Technology, Kharagpur-721302, India*
[2]*Department of Chemical Engineering, Pohang University of Science and Technology (POSTECH), Kyungbuk 790-784, South Korea*

Received 4 February 2010; accepted 13 July 2010
DOI 10.1002/app.33057
Published online 22 September 2010 in Wiley Online Library (wileyonlinelibrary.com).

ABSTRACT: A novel method of developing cocontinuous morphology in 75/25 and 80/20 *w*/*w* polypropylene/high density polyethylene (PP/HDPE) blends in the presence of small amount (0.5 phr) of organoclay has been reported. SEM study indicated a reduction in average domain sizes (*D*) of disperse HDPE when PP, HDPE, and the organoclay were melt-blended simultaneously at 200°C. However, when the two-sequential heating protocol was employed, (that is, the organoclay was first intercalated by HDPE chains at 150°C, followed by melt blending of PP at 200°C), very interestingly a cocontinuous morphology was found even for very asymmetric blend compositions. WAXD study revealed the intercalation of both PP and HDPE chains inside the clay galleries, when PP/HDPE and clay were melt-mixed together at 200°C. However, when the two-sequential heating protocol was used the organoclay platelets were selectively intercalated by the HDPE chains. Addition of SEPS in the blend decreased the *D* of HDPE domains in both the blending methods. Thus, the observed cocontinuous morphology in asymmetric composition of PP/HDPE blend in presence of clay is because of the barrier effect of the clay platelets in the HDPE phase that restrict the phase inversion into the domain/matrix morphology. © 2010 Wiley Periodicals, Inc. J Appl Polym Sci 119: 3080–3092, 2011

Key words: blends; cocontinuous morphology; intercalation; matrix; organoclay

INTRODUCTION

The blending of conventional polymers has been extensively employed to develop new polymeric materials. However, because of unfavorable enthalpy of mixing for two polymers, most polymer blends are immiscible, and thus form phase-separated morphology.[1,2] Depending on the blending composition and viscoelastic properties of each blend component, immiscible polymer blends show generally two types of the morphology: dispersed domain structure in the matrix phase and cocontinuous structure.[2,3] Asymmetric blend compositions show the former-type morphology, namely, the minor component forms the dispersed phase in the continuous phase of the major component.

Recently, the formation of the cocontinuous morphology has become important in polymer blends, especially for the development of the polymeric materials with high barrier properties. The cocontinuous structure is anticipated for immiscible polymer blends when the following condition is met[4,5]:

$$\phi_A/\eta_A \sim \phi_B/\eta_B \quad (1)$$

where ϕ_i and η_i (i = A and B) are the volume fraction and the viscosity of the component i. For immiscible polymer blend with $\eta_B/\eta_A >> 1$ (or $\phi_A/\phi_B >> 1$), the component B forms the dispersed domains in the matrix of A. On the other hand, immiscible polymer blends with $\eta_B/\eta_A \sim 1$ show the cocontinuous morphology for nearly symmetric compositions or blend compositions where the weight fraction of a minor component is not smaller than ~ 35 wt %. However, there is an increasing need for the generation of the cocontinuous morphology even for asymmetric blend composition where the minor component is less than 30 wt %. Although some research groups showed the cocontinuous morphology for asymmetric blend composition, the morphology did not represent the equilibrium state.[5,6–12]

Recently, several research groups[13–22] have investigated the role of nanoclay on the morphology of immiscible polymer blends. For instance, Gelfer et al.[13] reported that the preferential location of clay in PMMA phase increased the viscosity of PMMA that lowered the dispersed PS domain sizes in 50/50 *w*/*w* PS/PMMA blend. Wang et al.[14] reported that cointercalated polypropylene (PP) and PS chains inside the same clay galleries played the role of

Correspondence to: Dr. B. B. Khatua (khatuabb@matsc.iitkgp.ernet.in).

compatibilizer in 70/30 *w/w* PP/PS blend with clay, which reduced the disperse PS domain sizes. Sinha Ray and Bousmina[15,16] reported improved miscibility between polycarbonate (PC) and PMMA in PC/PMMA blends in the presence of organoclay. Voulgaris and Petridis [17] reported that the surfactants presented in organoclay played the role of emulsifier that decreased the PS domain sizes in 25/75 *w/w* polystyrene/poly(ethyl methacrylate) (PS/PEMA) blend-clay nanocomposites. Khatua et al.[18] reported that presence of exfoliated clay platelets in nylon 6 phase prevented the coalescence of dispersed EPR domains during mixing, which decreased the domain sizes of EPR phase in 80/20 *w/w* nylon 6/EPR blend. Li and Shimizu[19] reported the formation of cocontinuous structure in 50/50 *w/w* poly(phenylene oxide) (PPO)/polyamide 6 (PA6) blend in the presence of 5 wt % organoclay selectively dispersed in the PA6 phase. The increase viscosity of PA6 phase in presence of clay restricted the coalescence of PPO domains during melt mixing that changed the matrix-droplet morphology of the blend to a co-continuous structure. Mantia and coworkers[20] reported the formation of highly elongated PA6 domains in high density polyethylene (HDPE) matrix when 75/25 *w/w* HDPE/PA6 blend with 5 phr of organoclay was immediately cooled from the extrusion temperature. Interestingly, when the extruded pellets were compressed between the parallel plates of the rheometer, the morphology became a cocontinuous structure because of the connection of the elongated domains after the melting. Fu and coworkers[21] reported that the sea-island morphology of 60/40 *w/w* poly(*p*-phenylene sulfide) (PPS)/polyamide 66 (PA66) blend changed to cocontinuous structure when 10 wt % organoclay was selectively dispersed in the PA66 phase. They assumed that adsorption of PA66 onto the edge-contacted network structure of clay promoted the cocontinuous structure in the blend. Zhang et al.[22] reported that the increase in the viscosity of PBT phase present in clay (>2 wt %) changed the droplet morphology of 40/60 *w/w* PBT/PE blend into a cocontinuous one.

In summary, reports on immiscible polymer blend-clay nanocomposites indicated a reduction in disperse domain sizes, mostly for asymmetric blend compositions, by increasing the viscosity of the matrix phase in the presence of clay that prevented the coalescence of the domains during melt blending. However, formation of cocontinuous morphology was reported[19–22] only for the symmetric or near symmetric composition of the blends at higher amount of clay. Here, we introduce a novel mixing protocol to develop highly stable cocontinuous structure in asymmetric PP/HDPE blend compositions. When a small amount (0.5 phr) of organoclay was selectively dispersed in the HDPE before the melting of the PP, 75/25 and 80/20 *w/w* PP/HDPE blends showed the cocontinuous morphology. On the other hand, when the blend in presence of clay was prepared by mixing all the components directly at 200°C, the cocontinuous morphology was not observed.

EXPERIMENTAL SECTION

Material details

Commercial grade PP (M110, MFI 10 g/10 min) and two different grades of HDPE (M5025L, MFI 30 g/10 min and M5018L, MFI 19 g/10 min) were received from Haldia Petrochemicals, India. The high viscosity (MFI 19 g/10 min) HDPE is referred to as HDPE-h. Polystyrene-*block*-poly(ethylene-ran-propylene)-*block*-polystyrene (SEPS, Kraton G1702) was obtained from Kraton Polymers, USA. PE-*graft*-maleic anhydride copolymer (PE-*g*-MA) (A-C® 575P) was supplied by Honeywell, USA. Cloisite 20A, a modified montmorillonite, was supplied by Southern Clay Pdt., USA. It is a montmorillonite modified with dimethyl dihydrogenated tallow ammonium to increase the layer spacing (*d*) of Na^+-montmorillonite. The cation exchange capacity (CEC) of Cloisite 20A is 95 mequiv./100 g. Hereafter, Cloisite 20A is referred to as the clay.

Preparation of blends

Four different compositions (75/25, 80/20, 85/15, and 25/75 *w/w*) of PP/HDPE blends with various amounts (0–5 phr) of SEPS and (or) organoclay were prepared by melt mixing in an internal mixer (Brabender Plasticorder) having a capacity of 50 cc. All polymers and the clay were completely dried in a vacuum oven at 80°C for 36 h prior to melt blending. Two different blending methods were used for melt blending.

Method 1

Desired amounts of PP, HDPE, and SEPS or the clay were dry-mixed and then fed together into the internal mixer. Mixing was carried out at 200°C, 60 rpm for 15 min. Blend of 75/25 *w/w* PP/HDPE was also prepared without SEPS and the clay for the reference. Finally, all the blends were compression-molded in a hot press at 200°C under constant pressure (20 MPa) for further characterizations.

Method 2

Desired amounts of PP, HDPE, and SEPS or the clay were dry-mixed and fed into the internal mixer maintained at ~ 150°C (above the melting temperature of HDPE but below the melting point of PP), and mixing was carried out for 10 min. Then, the temperature of the internal mixer was increased to

200°C for ~ 10 min, and the mixing was performed at this temperature for 15 min at a constant rotating speed of 60 rpm. Blends of 75/25 *w/w* PP/HDPE without SEPS and clay were also prepared for the reference. All the blends were compression-molded in a hot press at 200°C under constant pressure (20 MPa) for further characterizations.

CHARACTERIZATIONS

X-ray diffraction study

The gallery height (*d*-spacing) of neat clay itself as well as the clay in PP/HDPE blends was measured by using a wide angle X-ray diffractometer, (WAXD, Rigaku, Ultima-III, Japan) with nickel-filtered CuKα line (=0.15404 nm) operated at 40 kV and 100 mA, and at a scanning rate of 0.5°/min. The sample-to-detector distance was 400 mm.

Morphology

The morphology of the PP/HDPE blends, without and with SEPS or the clay, was studied with the scanning electron microscope, SEM, (VEGA II LSU, TESCAN, Czech Republic) operated at an accelerating voltage of 5 kV (or 10 kV). The specimens were carefully broken under liquid nitrogen atmosphere. Then, the specimens were coated with a thin layer of gold to avoid electrical charging and SEM images were taken on the fractured surface.

The number–average domain diameter (D_n) was calculated with Scion Image analyzer software (Scion Corp., USA). The cross-sectional area (A_i) of each domain in the SEM micrograph was measured and then converted into the diameter (D_i) of a circle having the same cross-sectional area by using the following equations.

$$D_i = 2(A_i/\pi)^{\frac{1}{2}} \quad (2)$$

$$D_n = \sum N_i D_i \Big/ \sum N_i \quad (3)$$

where N is the number of dispersed domains in the SEM micrograph.

TEM analysis

The location of the clay platelet in the PP/HDPE blends was studied by transmission electron microscopy (HRTEM: JEM-2100, JEOL, Japan) operating at an accelerating voltage of 200 kV. The clay nanocomposite samples were ultramicrotomed under cryogenic condition with a thickness of 60–80 nm. Since the clay has much higher electron density than neat polymers, it appeared dark in TEM images.

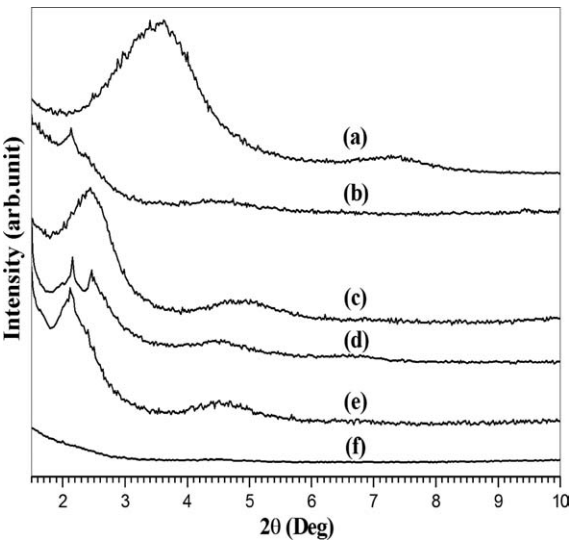

Figure 1 WAXD patterns of neat clay (a), HDPE/clay (b), PP/clay (c), and 75/25 *w/w* PP/HDPE blend/clay nanocomposites prepared by two different mixing methods: (d) method-1, (e) method-2, and (f) 75/25 *w/w* PP/HDPE blend-clay nanocomposites with 3 phr PE-g-MA, prepared by method-2. The amount of the clay in all the nanocomposites was 0.5 phr.

RESULTS AND DISCUSSION

WAXD analysis

Figure 1 shows the WAXD profiles of neat clay and the clay in three different nanocomposites (HDPE/clay, PP/clay, and 75/25 *w/w* PP/HDPE blend/clay) prepared by two different mixing methods. The neat clay showed the characteristic peak at a 2θ of 3.62°, corresponding to the *d*-spacing of 24.38 Å. In all the nanocomposites, the characteristic peak for the clay was shifted to lower angle, indicating the intercalation of the polymer chains inside the clay galleries. For instance, the appearance of the peak at a 2θ of 2.12° in HDPE/clay and 2.44° in PP/clay nanocomposites indicated the intercalation of HDPE and PP chains inside the clay platelets with *d*-spacings of 41.63 Å and 36.17 Å, respectively. In the blend/clay nanocomposites prepared by the mixing method-1, two distinct peaks for the clay were observed at 2θ of 2.14° and 2.45°, corresponding to the *d*-spacing of 41.24 Å and 36.02 Å, respectively. This result clearly indicated that both the HDPE and PP chains were intercalated into the clay galleries in the blend/clay nanocomposites.

Interestingly, the blend/clay nanocomposites prepared by the mixing method-2 did not show any peak at 2θ ~ 2.45°, indicating the lack of the intercalation of the clay by the PP chains. The appearance of the peak at a 2θ ~ 2.10° indicated the intercalation of the clay by the HDPE chains only. Thus, we assume that in the blend/clay nanocomposites prepared by the method-2, melting of HDPE prior to

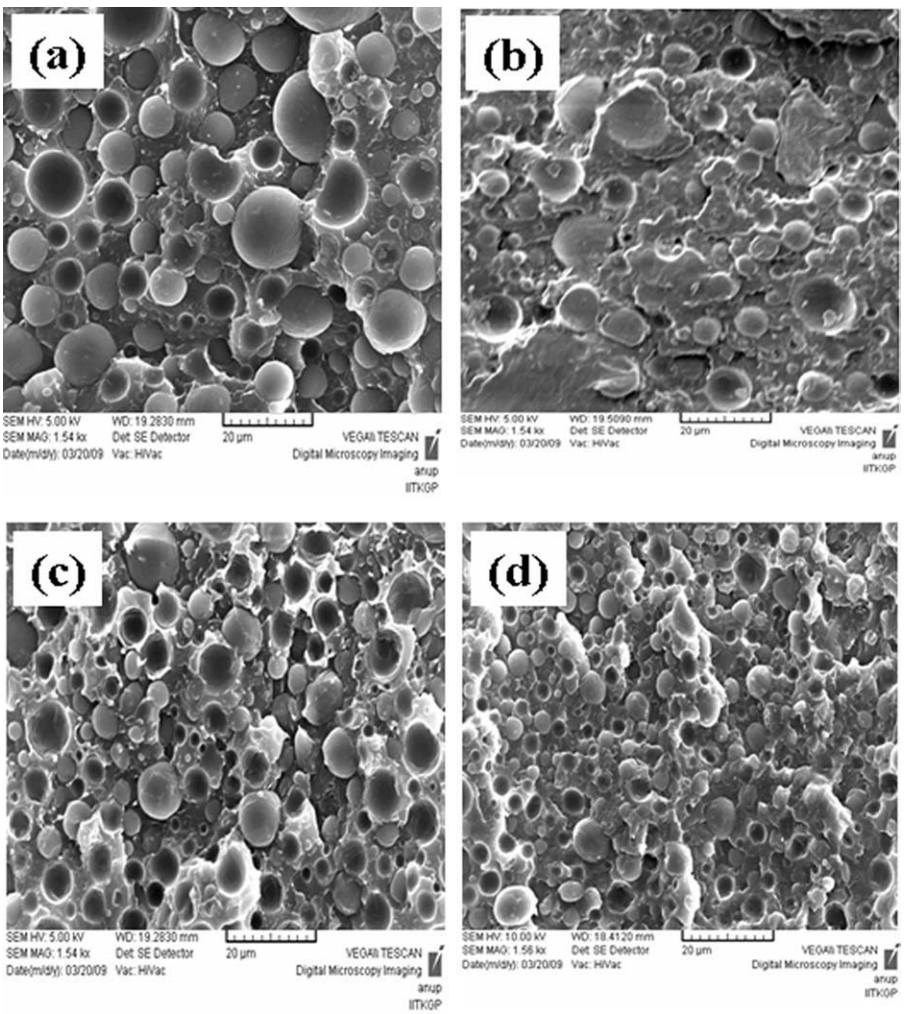

Figure 2 SEM images of the 75/25 *w*/*w* PP/HDPE blends with SEPS and clay prepared by method-1: (a) neat blend, (b) 0.5 phr SEPS, (c) 0.5 phr clay, (d) 1 phr clay.

the melting of PP, promoted selective intercalation of HDPE chains inside the clay platelets. When HDPE/PP/clay nanocomposite with 3 phr PE-g-MA was prepared by mixing method-2, no characteristic clay peak was observed. This indicated that the clay platelets were exfoliated by the HDPE chains. PE-*g*-MA is well known to promote the exfoliation of the clays in HDPE matrix.[23,24]

Morphology study

Figure 2 represents the SEM images of the 75/25 *w*/*w* PP/HDPE blends without and with SEPS or the clay prepared by the method-1. The SEM image of the PP/HDPE blend without SEPS and the clay clearly demonstrated a two-phase matrix-particle microstructure. The minor phase (HDPE) dispersed as spherical domains in PP matrix [Fig. 2(a)]. In addition, the microvoids surrounding the HDPE droplets indicated weak interfacial adhesion in the blend. Because of the high interfacial tension between the two polymers, the spherical morphology is anticipated because of the minimization of the interfacial area.[25–29] It was observed that D_n of the dispersed HDPE phase ($\sim$ 6.46 μm) in PP/HDPE blend decreased to $\sim$ 3.82 μm when 0.5 phr SEPS was added [Fig. 2(b)] in the blend. SEPS acts as a compatibilizer for this blend system, as reported elsewhere.[30]

Interestingly, addition of small amount (0.5 phr) of the clay to the blend resulted in a great decrease in D_n of the dispersed HDPE phase [$\sim$ 2.96 μm; see Fig. 2(c)]. With increasing the clay content to 1 phr, D_n of the blend further decreased to 2.02 μm (Fig. 2 days). This indicates that the presence of clay platelets restricted the coalescence of the dispersed domains in the PP/HDPE blend. However, in contrast to the PP/HDPE/SEPS blend, the blend/clay nanocomposites showed poor interfacial adhesion. Thus, the mechanism for the decrease in D_n of dispersed domains in presence of the clay was different from that with SEPS in the blend. We assume that, the intercalated clay platelets in the matrix phase prevented the coalescence of dispersed domains,

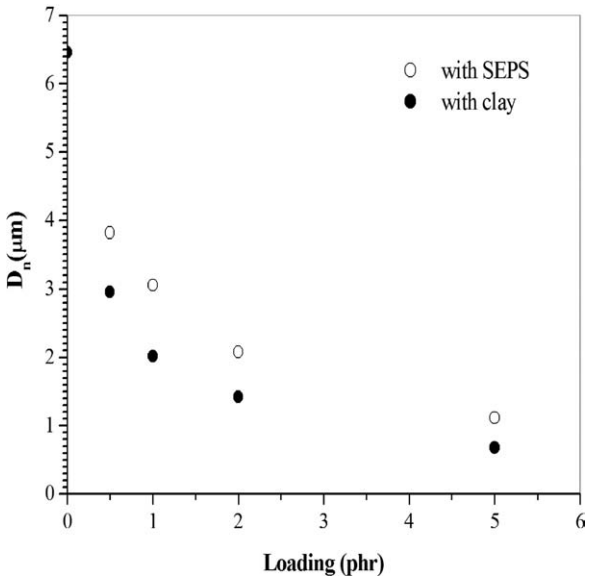

Figure 3 Plot of D_n versus various amounts of SEPS and clay in 75/25 w/w PP/HDPE blends, prepared by method-1.

whereas SEPS acted as a physical compatibilizer for making entanglement or bridging of different polymer chains at the interface of the blend.

On the basis of SEM images, plots of D_n versus the amount of SEPS or the clay are shown in Figure 3. As observed, a rapid decrease in D_n of the blend was found at lower amounts of the clay and then a slow but gradual decrease in D_n was observed with further increasing the amount of the clay. This result is consistent with the earlier report.[20] The change in D_n with the amount of clay in the blend was very similar to the 75/25 w/w PP/HDPE blend with various amounts of SEPS. This trend of decreasing D_n is very similar to the emulsification curve, which has been reported for an immiscible blend with a block (or graft) copolymer.[31]

Figure 4 represents the SEM images of the blends with different amount of clay and SEPS, prepared by the method-2. Very interestingly, the dispersed domain/matrix-morphology changed to cocontinuous structure when only a small amount of clay (0.5 phr) was added [Fig. 4(a)]. As the clay content was increased to 1 phr, cocontinuous morphology of the blend was more evident [Fig. 4(b)]. On the other hand, the morphology of the 75/25 w/w PP/HDPE blend with 1 phr SEPS, even though it was prepared by the method-2, showed the dispersed domain/matrix morphology, where HDPE dispersed as spherical domains [Fig. 4(c)]. In this situation, the average size of the dispersed HDPE domains was very similar to that of 75/25 w/w PP/HDPE blend with 1 phr SEPS, prepared by the method-1. Thus, for both method-1 and method-2, SEPS played only the role of a compatibilizer and failed to promote the cocontinuous structure of the blend. This observation led us to conclude that the cocontinuous morphology developed in the blend-clay nanocomposites was because of the change in heating protocol in method-2 that changed the sequence of clay intercalation during mixing.

It is known that the cocontinuous structure of a binary polymer blend can be formed within narrow blend compositions that are governed by the relative melt viscosities of the two components.[5,32–37] It has been reported that the presence of the clay platelets affects the rheological behavior of polymers. With increasing the extent of the intercalation of the clay platelets, the melt viscosity of the polymer increases and shear thinning behavior is more evident at high shear rates.[38,39] In the present study, the clay platelets were selectively intercalated and dispersed in the HDPE phase in PP/HDPE blend when the blend was prepared by the method-2. However, because of very small amount (0.5 phr) of the clay, the increase in the viscosity of HDPE phase was only marginal. Therefore, the cocontinuous morphology induced by the addition of the clay was because of the barrier effect of the intercalated clay platelets in HDPE phase, which prevented the phase coalescence during melt mixing and thereby stabilizing the structure formed at initial stage of mixing.

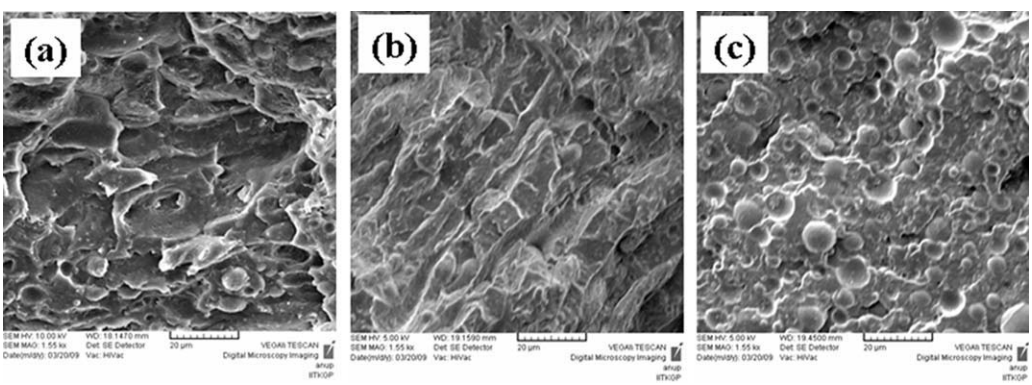

Figure 4 SEM images of the 75/25 w/w PP/HDPE blends with clay and SEPS, prepared by method-2: (a) 0.5 phr clay, (b) 1 phr clay, and (c) 1 phr SEPS.

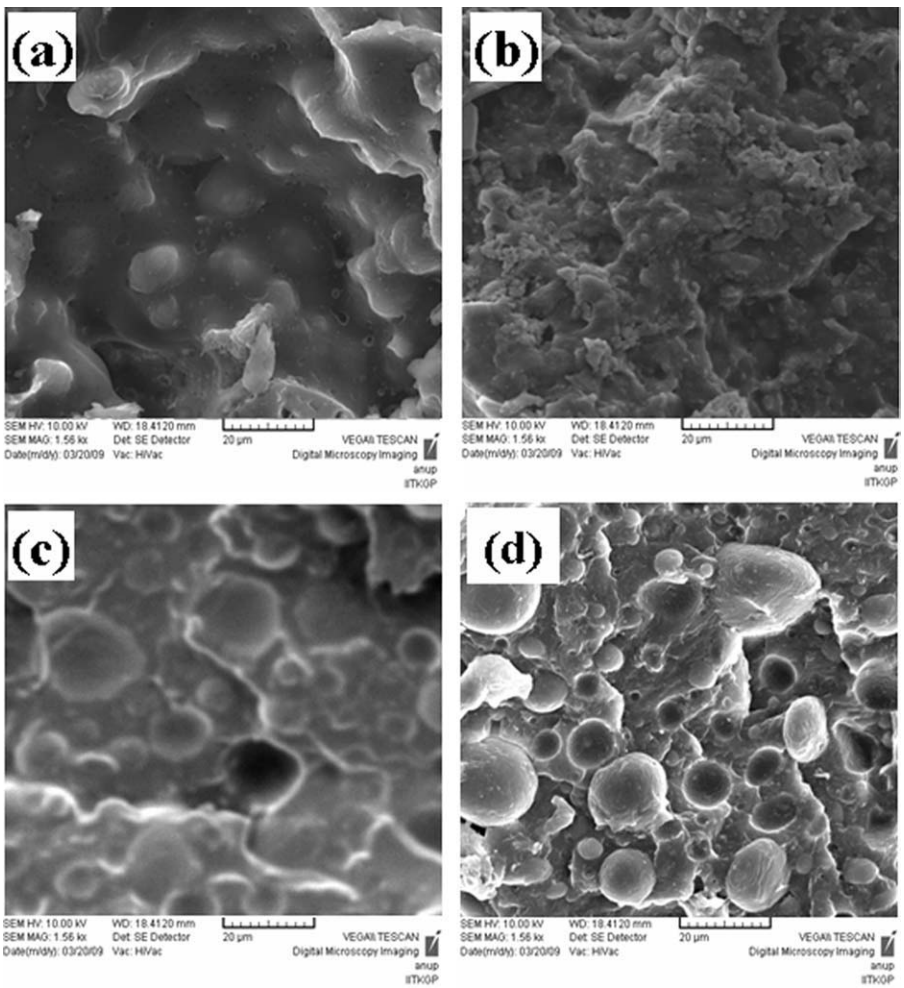

Figure 5 SEM images 75/25 w/w PP/HDPE blends without the clay at different mixing times after reaching the mixing temperature at 180°C during the blending by method-2: (a) 2 min, (b) 5 min, (c) 10 min, and (d) 15 min.

The development of morphology in 75/25 w/w PP/HDPE blend without and with clay has been investigated in detail with the mixing time. Figure 5 represents the SEM images of the blends without any clay, at different mixing times, prepared by method-2. Since the melting temperature (T_m) of PP (180°C) is higher than the T_m of HDPE (130°C), in method-2, HDPE melted first formed the matrix phase and PP pellets were suspended in the HDPE matrix. As the temperature reached 180°C, PP pellets started melting and remained as dispersed phase until they touched each other. With increase in mixing time, the PP phases combined together to form the continuous phase and phase inversion took place. Finally, the minor phase HDPE formed the droplets and were dispersed in the continuous PP matrix. The higher volume fraction and melt viscosity of PP in 75/25 w/w PP/HDPE blend composition resulted in the formation of this droplet morphology of HDPE in the PP matrix.

Interestingly, the development of phase morphology in the blend-clay nanocomposites prepared by method-2 was found to change dramatically compared with that without any clay. Figure 6 represents the SEM images of the blend in presence of 0.5 phr clay at different mixing times. Here, the clays were allowed to intercalate selectively by the HDPE chains in the first stage of mixing. In contrast to Figure 5(a), PP pellets were suspended in the intercalated HDPE–clay nanocomposites matrix until the temperature reached the T_m of PP [Fig. 6(a)]. With increasing mixing time, PP started to melt and was deformed into elongated structures [Fig. 6(b)]. At 10 min of mixing, dispersed PP phases were more elongated and dispersed phase was still observed. The PP phases did not contact each other, and the continuous structure was not formed yet [Fig. 6(c)]. Finally, a cocontinuous structure of HDPE and PP was found in the blend-clay system at 15 min of the mixing (Fig. 6, days). We propose that the intercalated clay platelets in the HDPE matrix might have restricted the movement of PP droplets and hence prevented the coalescence of the PP phases to form the continuous matrix phase by phase inversion process.

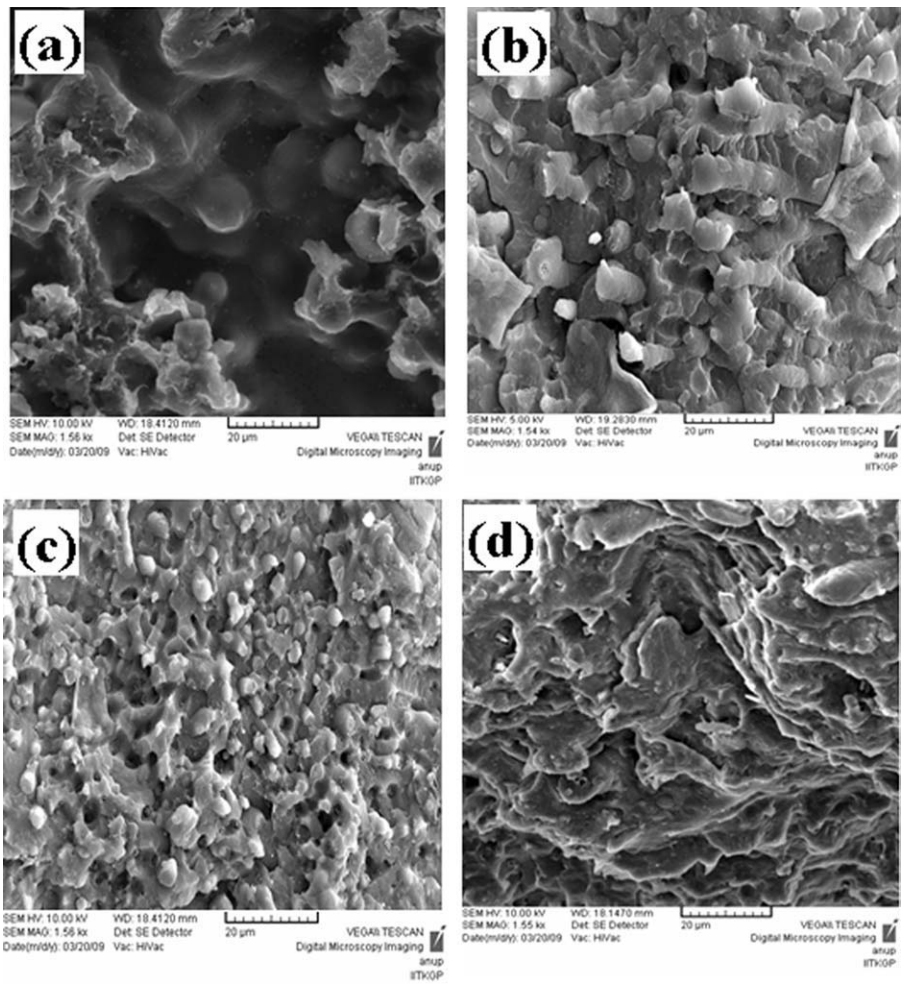

Figure 6 SEM images of 75/25 *w*/*w* PP/HDPE blends with 0.5 phr clay at different mixing times after reaching the mixing temperature at 180°C during the blending by method-2: (a) 2 min, (b) 5 min, (c) 10 min, and (d) 15 min.

If the above scenario for the role of clay is reasonable, then one can expect formation of highly cocontinuous structure in the presence of exfoliated clay platelets in the HDPE phase prior to the melting of PP during mixing. For that purpose, we prepared the 75/25 *w*/*w* PP/HDPE blend-clay nanocomposites in presence of 3 phr PE-*g*-MA by the method-2. Addition of PE-*g*-MA promoted the exfoliation of clay platelets in the HDPE phase (Fig. 1). Figure 7 represents the SEM images of the blend-clay nanocomposites with PE-*g*-MA. It is seen that the extent of cocontinuous morphology in the blend-clay nanocomposites [Fig. 7(a)] with PE-*g*-MA was increased compared to that without PE-*g*-MA. Again, the cocontinuous morphology of the blend was highly stable even after 30 min of mixing at stage-2 [Fig. 7(b)]. This observation indicated that compared with intercalated clays, exfoliated clay platelets in the minor phase (HDPE), prior to the melting of major phase (PP), were more effective in promoting cocontinuous morphology in 75/25 *w*/*w* PP/HDPE blend. We also investigated the morphology of 75/25 *w*/*w* PP/HDPE blend with 3 phr PE-*g*-MA, prepared by the method-2 without the clay. However, absence of the clay in this blend indicated the formation of dispersed domain/matrix-morphology, where HDPE was dispersed as domains in the PP matrix [Fig. 7(c)]. Furthermore, when the blend-clay with PE-*g*-MA was prepared by method-1, we could not see any cocontinuous structure [Fig. 7(d)], which was similar to the morphology of pure PP/HDPE blend [Fig. 2(a)] prepared by method-1. A slight increase in D_n of the dispersed HDPE domains was because of the presence of PE-*g*-MA that selectively exfoliated the clays in the HDPE domains, and hence increased the melt viscosity of HDPE.

Effect of minor phase viscosity on blend morphology

In 75/25 *w*/*w* PP/HDPE blend with 0.5 phr of the clay prepared by method-2, clays were mostly intercalated/dispersed in the HDPE phase, as evident from the WAXD study. Thus, assuming all the clays

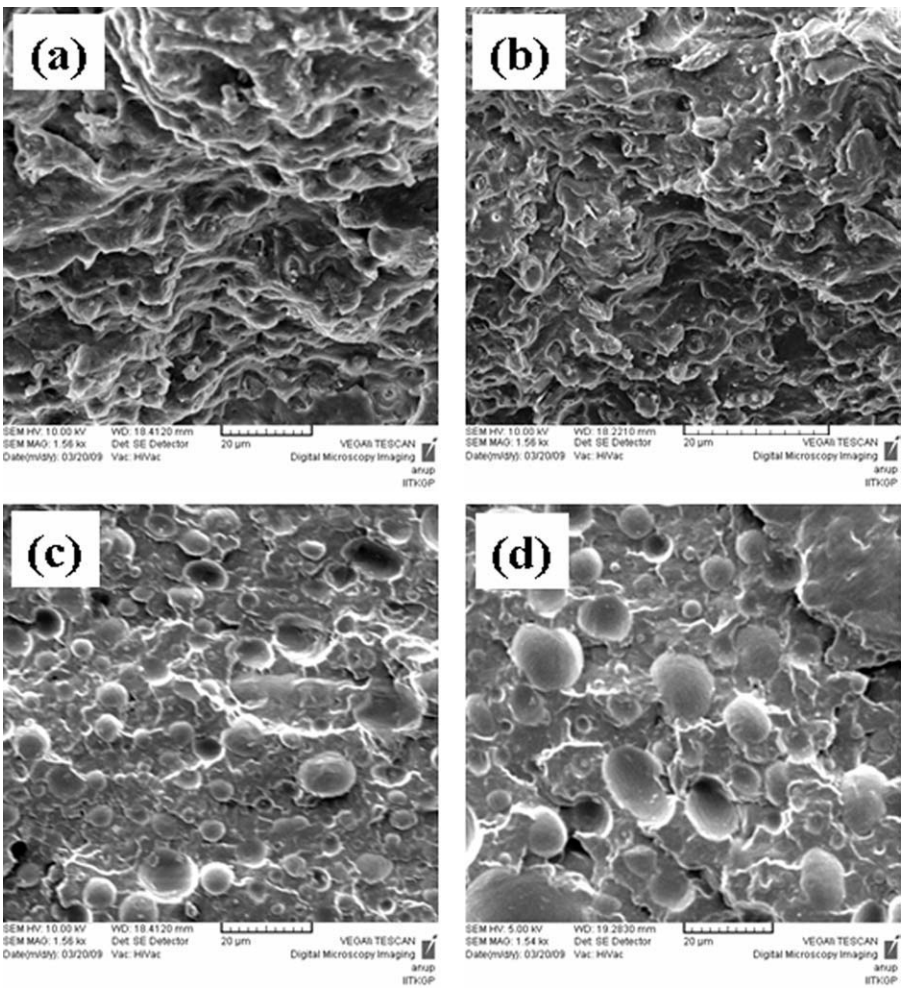

Figure 7 SEM images of the 75/25/3 *w/w* PP/HDPE/PE-g-MA blends with 0.5 phr clay at different mixing times during the blending by method-2: (a) 15 min, (b) 30 min; (c) without any clay, 15 min; and (d) with 0.5phr clay prepared by method-1, with mixing time of 15 min.

selectively dispersed in HDPE, the effective clay loading in HDPE in the blend was 2 phr. We measured the complex viscosity (η*) of neat PP, HDPE, HDPE-clay (2 phr), and 75/25 *w/w* PP/HDPE blend with 0.5 phr clay. As observed in Figure 8, the addition of 2 phr clay slightly increased the viscosity of HDPE. This implied that the D_n of HDPE in 75/25 *w/w* PP/HDPE blend-clay (0.5 phr) nanocomposites would increase slightly when all the clays were located in HDPE phase. However, a decrease in D_n was observed (Fig. 2) when the blend was prepared by method 1 in presence of 0.5 phr clay. This can be explained in terms of the change in viscosity ratio of PP and HDPE induced by the intercalation of the clay in the blend-clay nanocomposites. Since the clay did not have any special affinity to intercalate with either PP or HDPE in the blend prepared by method-1 (Fig. 1), we assume that most of the clays in 75/25 *w/w* PP/HDPE blend were located in the PP phase because of a higher volume fraction of PP. Thus, D_n of the blend was decreased because of the

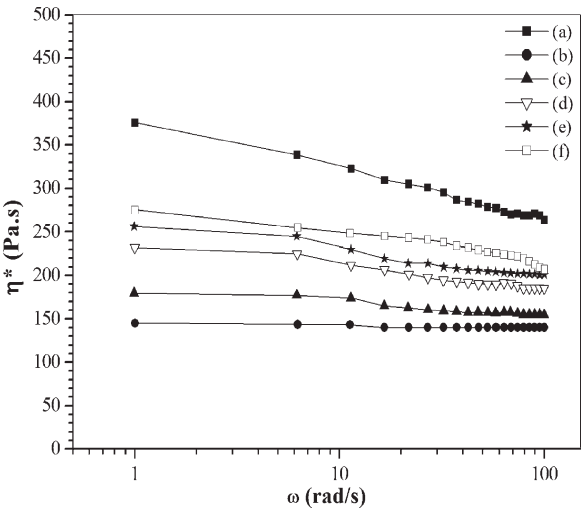

Figure 8 Plot of complex viscosity (η^*) with frequency (ω) at 200°C: (a) PP, (b) HDPE, (c) HDPE-clay (2 phr), (d) HDPE-h, (e) 75/25 *w/w* PP/HDPE blend with 0.5 phr clay, (f) 75/25 *w/w* PP/HDPE-h blend without any clay.

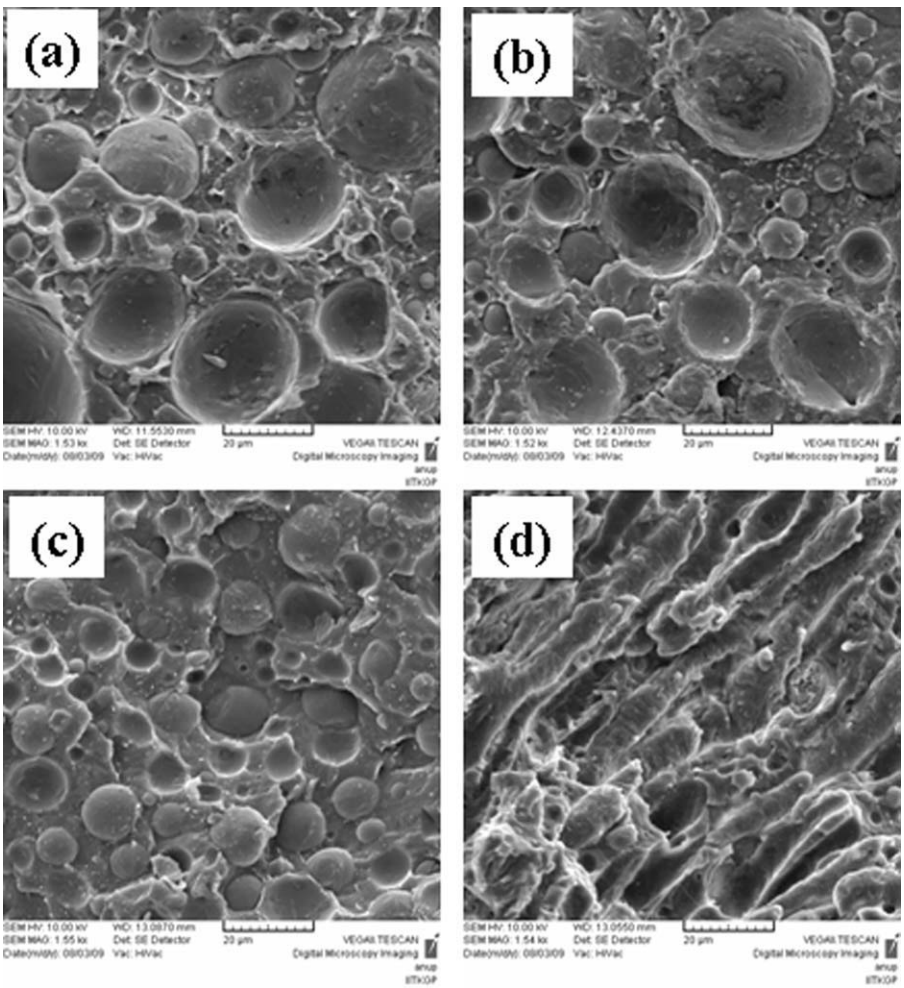

Figure 9 SEM images of the 75/25 *w*/*w* PP/HDPE-h blends without (a, b) and with 0.5 phr clay (c, d), prepared by two methods: (a, c) method-1; (b, d) method-2.

barrier effect of the clay in matrix phase (PP), as well as decrease in the viscosity ratio of HDPE and PP in presence of clay.

Now, one can argue whether the observed of cocontinuous structure in the blend-clay system prepared by method-2 was because of the viscosity effect of HDPE or the presence of the clay. To check this possibility, we also prepared the 75/25 *w*/*w* PP/HDPE blend with another high viscosity HDPE (HDPE-h). The viscosity of 75/25 *w*/*w* PP/HDPE-h blend appeared almost similar to that of 75/25 *w*/*w* PP/HDPE blend with 0.5 phr clay throughout the entire frequencies (0.1–100 rad/s).

Figure 9 shows the SEM images of 75/25 *w*/*w* PP/HDPE-h blend without and with the clay, prepared by two melting methods. Regardless of the melting method, in 75/25 *w*/*w* PP/HDPE-h blends without any clay, HDPE-h was dispersed as spherical domains in the PP matrix [Fig. 9(a,b)], similar to that of PP/HDPE blend. D_n of dispersed HDPE-h was significantly increased (more than 12 μm) as compared with the D (∼ 6.46 μm) with low viscosity HDPE. This was because of the higher viscosity of HDPE-h, compared with the HDPE. However, a slight decrease in D_n of HDPE-h was observed when the blend was prepared by method 1 in presence of 0.5 phr clay [Fig. 9(c)]. Interestingly, the droplet morphology of 75/25 *w*/*w* PP/HDPE-h blend with 0.5 phr clay was changed to cocontinuous structure when blending was done by method 2 [Fig. 9(d)]. These observations lead us to conclude that the increased viscosity of the minor phase (HDPE) by the clay was not a main factor in developing the cocontinuous structure. The presence of the intercalated clay platelets in HDPE phase, prior to the melting of PP phase, prevented the coalescence of the PP phases that promoted the formation of cocontinuous morphology in 75/25 *w*/*w* PP/HDPE blends.

To investigate the effect of low viscosity of the dispersed PE phase on phase morphology of PP/HDPE blend-clay nanocomposites, we studied the 75/25 *w*/*w* PP/LLDPE blend with very low viscosity LLDPE (Relene® M26500 from Reliance Industries; MFI 50 g/10 min). Figure 10 represents the SEM images of the

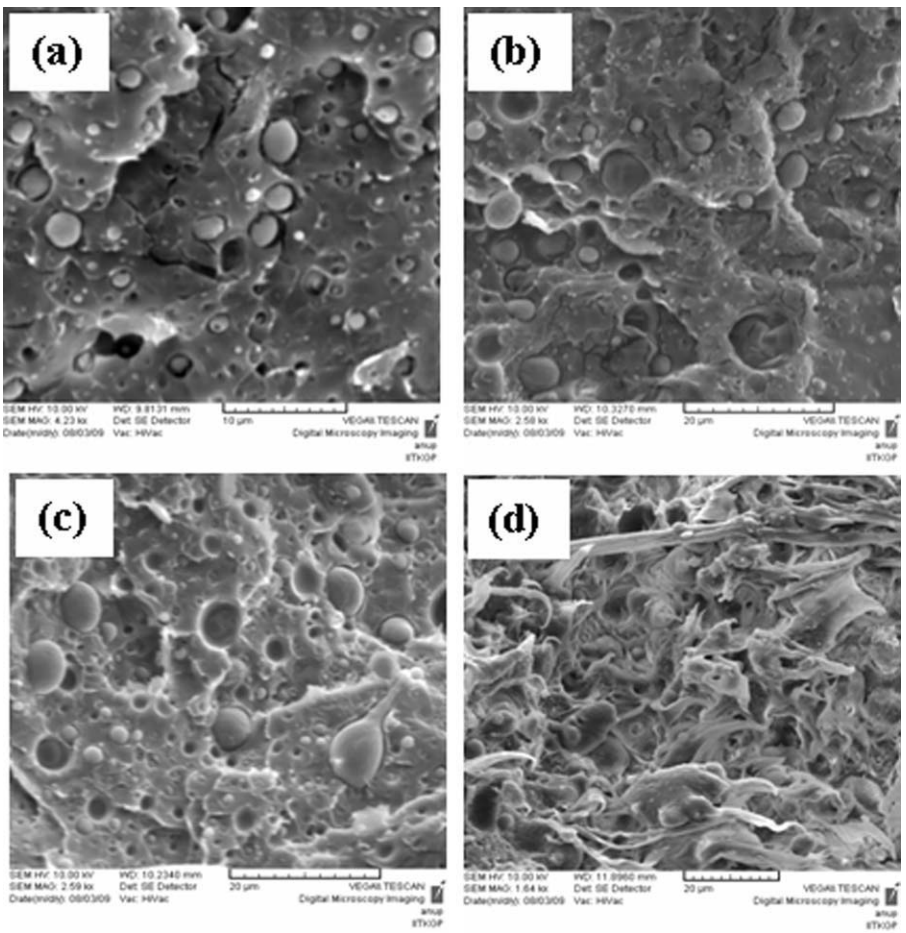

Figure 10 SEM images of 75/25 *w/w* PP/LDPE blends without (a and b) and with 0.5 phr clay (c and d) prepared by two methods: (a, c) method-1; (b, d) method-2.

blends without and with 0.5 phr clay. As observed, the droplet morphology was formed in the blend without [Fig. 10(a)] and with the clay [Fig. 10(c)] when mixing was done by method-1. Interestingly, intercalation of the clays in PE phase prior to the melting of PP showed the cocontinuous morphology (Fig. 10 days) even for the 75/25 *w/w* PP/LLDPE blend with 0.5 phr clay prepared by method-2. This observation clearly showed the role of intercalated clays in promoting cocontinuous structure in the blend when the minor phase is allowed to melt, prior to the melting of major phase during melt mixing.

TEM study

Figure 11 represents the TEM images of the 75/25 *w/w* PP/HDPE blends with 0.5 phr of clay at different magnifications prepared by the method-2. The TEM images [Fig. 11(a,b)] revealed that in PP/HDPE/clay nanocomposite, the clay platelets were mostly located in the HDPE phase and not in the PP phase or at the interface. This might be because of the intercalation of the clays by the HDPE chains prior to the melting of PP during melt-mixing in method-2. Based on the TEM observation, a schematic for the location of clay platelets in the blend is shown in Figure 11(c). The dark portions in the schematic indicate the HDPE phase. We propose that the network structure of intercalated clay platelets in the minor phase (HDPE) played the role of physical barrier, and thereby prevented the coalescence of PP phases even after the melting of PP in method-2. Thus, the phase inversion process of PP to become a continuous phase and formation of dispersed HDPE droplets were prevented, and both phases formed a cocontinuous structure in the blend.

Morphology of highly asymmetric blend compositions

To check whether cocontinuous structure can also be observed with increasing the asymmetric compositions of PP/HDPE blend in presence of clay, we prepared 80/20 *w/w* and 85/15 *w/w* PP/HDPE blends by using two different mixing methods. Figure 12 represents the SEM images of 80/20 *w/w* PP/HDPE blends without and with clay. As observed, the

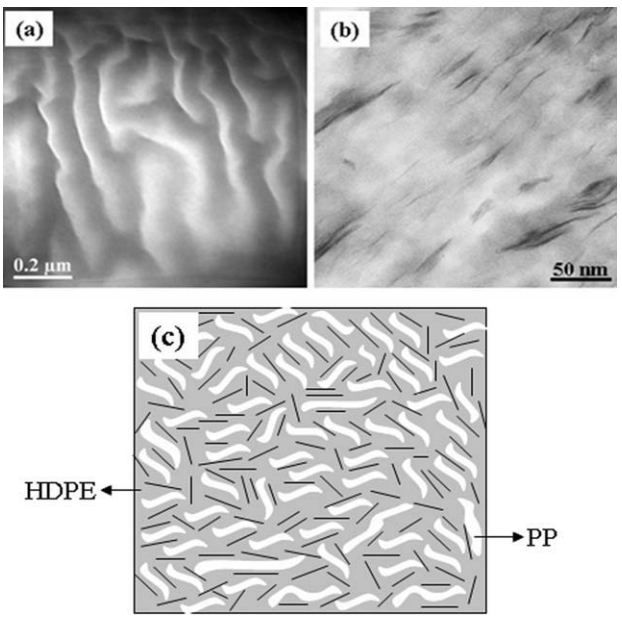

Figure 11 TEM images of the 75/25 *w/w* PP/HDPE blend with 0.5 phr clay: (a) lower magnification; (b) higher magnification; (c) schematic for the location of the clay platelets in the blend.

blend without or with 0.5 phr clay indicated the formation of droplet/matrix-morphology [Fig. 12(a,b)] when mixing was done by method-1. Interestingly, the cocontinuity was observed for 80/20 *w/w* PP/HDPE blend with 0.5 phr clay when the blend was prepared by method-2 [Fig. 12(c)]. However, 85/15 *w/w* PP/HDPE blend with 0.5 phr clay did not show the cocontinuous morphology in the entire sample even though it was prepared by method-2. In this situation, HDPE phases were dispersed mostly as spherical domains, although some regions still showed cocontinuous structure [Fig. 13(b)].

Melting sequences of PP and HDPE and blend morphology

To study the effect of melting sequence of PP and HDPE on the morphology of the blend prepared by method-2, we also investigated the morphology of 25/75 *w/w* PP/HDPE blends without and with 0.5 phr clay. In this composition, HDPE was the major phase, contrary to the 75/25 *w/w* PP/HDPE blend where HDPE was the minor phase. It's noteworthy that irrespective of the blending sequences 25/75 *w/w*, PP/HDPE blends only showed the matrix/droplet morphology without having cocontinuous structure, where PP was dispersed as domains in HDPE matrix (Fig. 14). The intercalation of the clay in HDPE matrix before melting the PP phase in method 2 significantly reduced the D_n of PP in the blend as compared with that prepared by method 1. The decrease in D_n of the blend in presence of the clay was because of the barrier effect of the intercalated clay platelets in HDPE matrix that prevented the coalescence of PP domains, and the increase in the viscosity of HDPE in presence of clay that decreased the viscosity ratio of PP and HDPE. A similar observation was reported by Paul and coworkers in PC/SAN and PBT/ABS blends with clay.[40,41] For 25/75 *w/w* PP/HDPE blend composition, the PP became minor phase in the molten HDPE (major phase) during the initial stage of mixing at 150°C in method 2. Thus, this minor phase maintained without the phase inversion because of the smaller volume fraction of PP, even at temperatures above the T_m of PP. This was in contrast to the 75/25 *w/w* PP/HDPE blend prepared by method 2, where the final morphology was formed through phase inversion process. Thus, the observed cocontinuous morphology in 75/25 *w/w* PP/HDPE blend-clay nanocomposites, prepared by method 2, was because of the presence of intercalated clays in the minor phase.

The above results clearly indicated that to generate the cocontinuous structure in asymmetric blend composition in presence of clay, the minor phase should have lower melting temperature (T_m) than that of the major phase. The barrier effect of the intercalated clay platelets in the minor phase, prior to the melting of the major phase, prevented

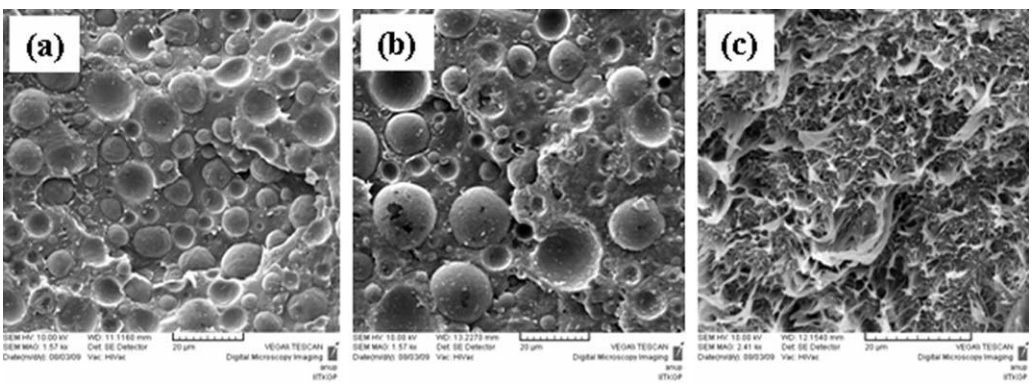

Figure 12 SEM images of 80/20 *w/w* PP/HDPE blends without and with 0.5 phr clay prepared by different mixing methods: (a) no clay, method-1; (b) 0.5 phr clay, method-1; (c) 0.5 phr clay, method-2.

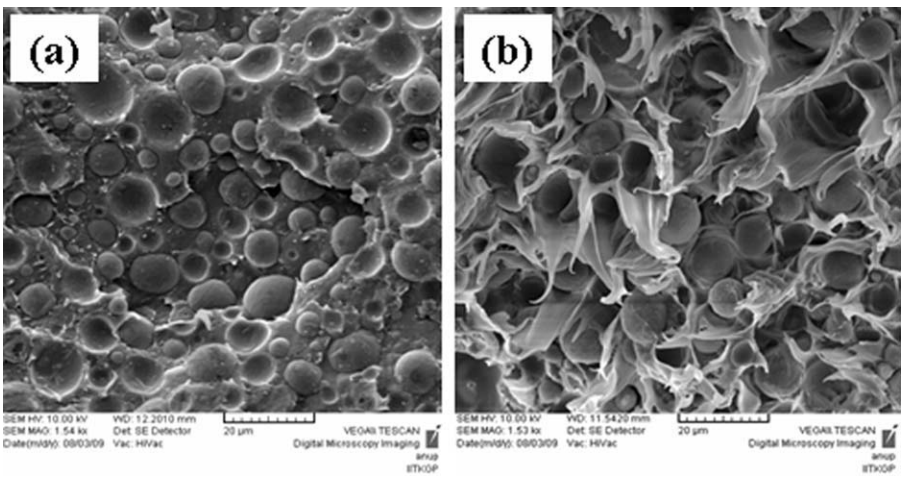

Figure 13 SEM images of 85/15 *w*/*w* PP/HDPE blends with 0.5 phr clay prepared by two methods: (a) method-1; (b) method-2.

the phase inversion process by restricting the coalescence of major phases during mixing. The increased viscosity of the minor phase by the clay did not play a major role in promoting cocontinuous structure.

CONCLUSIONS

The cocontinuous morphology in asymmetric compositions of PP/HDPE blend in the presence of

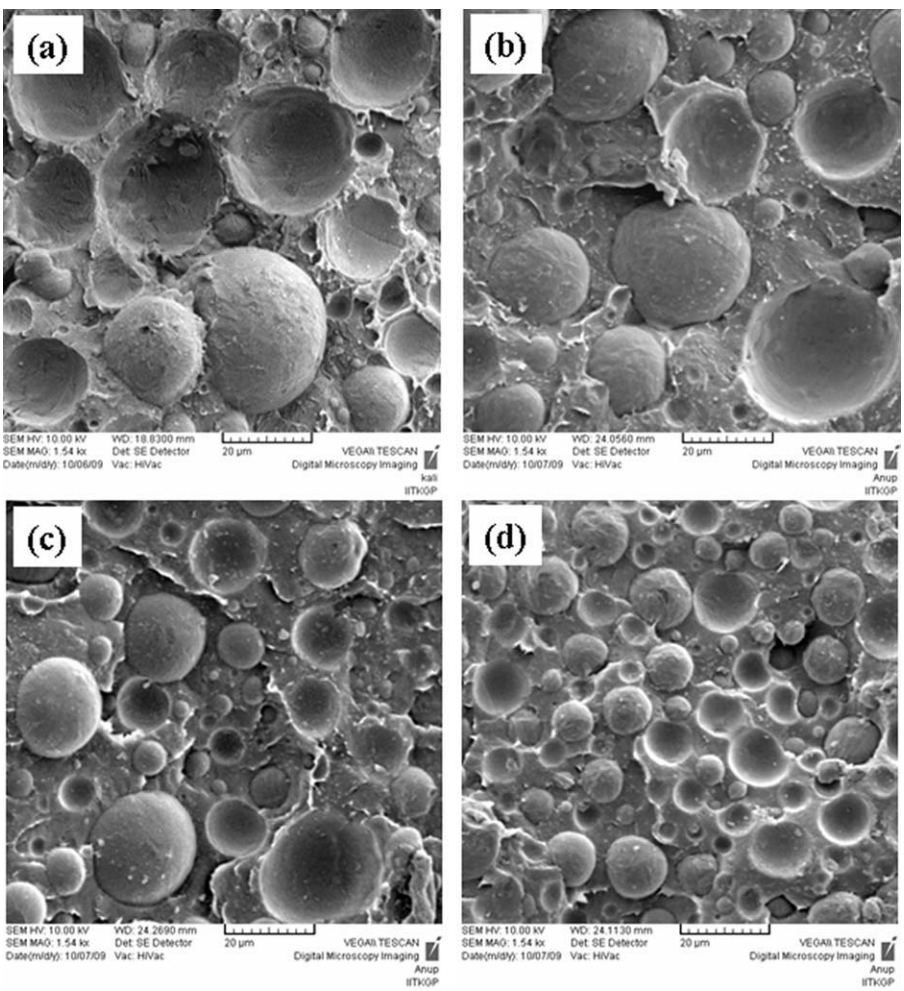

Figure 14 SEM images of the 25/75 *w*/*w* PP/HDPE-h blends without (a, b) and with 0.5 phr clay (c, d), prepared by two methods: (a, c) method-1; (b, d) method-2.

small amount (0.5 phr) of clay has been developed by changing the heating protocol during melt blending. Direct melt blending (method-1) of PP and HDPE at 200°C in the presence of clay (0.5 phr) significantly reduced the average domain sizes of HDPE in 75/25 *w/w* PP/HDPE blend than that of a physical compatibilizer (SEPS) at same loading. The intercalated clay platelets in the PP matrix played the role of a barrier that prevented the coalescence of dispersed HDPE domains during melt mixing. Interestingly, a slight change in the heating protocol in melt blending (method-2) that led to the melting of HDPE prior to the melting of PP resulted in the formation of cocontinuous morphology in 75/25 *w/w* and 80/20 *w/w* PP/HDPE blend in presence of 0.5 phr clay. WAXD study revealed the intercalation of the clays by the HDPE chains only when PP, HDPE, and clays were melt blended by method-2. Exfoliation of clay platelets in the HDPE phase by using PE-*g*-MA increased the extent of phase cocontinuity in (75/25 *w/w*) PP/HDPE blend, prepared by method-2. Irrespective of the heating sequences during blending, addition of PE-*g*-MA or SEPS decreased the average domain size of dispersed HDPE in the blends, and did not show any phase cocontinuity of PP and HDPE in absence of the clay. Moreover, 25/75 *w/w* PP/HDPE blend in presence of 0.5 phr clay showed the droplet/matrix structure, even when the blend was prepared by method-2. Thus, selective dispersion of clays in the minor phase (HDPE), prior to the melting of the major phase (PP) in method-2, restricted the phase inversion process that led to the formation of cocontinuous structure in 75/25 *w/w* and 80/20 *w/w* PP/HDPE blend with 0.5 phr clay.

References

1. Folkes, M. J; Hope, P. S. Polymer Blends and Alloys, 1st ed.; Blackie Academic and Professional, An imprint of Chapman & Hall: UK, 1993.
2. Utracki, L. A. Polymer Alloys and Blends; Hanser Publishers: Munich, 1989.
3. Paul, D. R. In Polymer Blends; Paul, D. R.; Newman, S., Eds., Vol. II; Academic Press: New York, 1978, p. 35.
4. Jordhamo, G. M.; Manson, J. A.; Sperling, L. H. Polym Eng Sci 1986, 26, 517.
5. Lee, J. K.; Han, C. D. Polymer 1999, 40, 6277.
6. Veenstra, H.; Van Dam, J.; Posthuma De Boer, A. Polymer 1999, 40, 1119.
7. Veenstra, H.; Norder, B.; Van Dam, J.; Posthuma De Boer, A. Polymer 1999, 40, 5223.
8. Mekhilef, N.; Favis, B. D.; Carreau, P. J Polym Sci Part B: Polym Phys 1997, 35, 293.
9. Willemse, R. C.; Doelam, R.; Gotsis, A. D. Proc Annu Tech Conf-ANTEC 1998, 2, 2556.
10. Tol, R. T.; Groeninckx, G.; Vinckier, I.; Moldenaers, P.; Mewis, J. Polymer 2004, 45, 2587.
11. Pötschke, P.; Paul, D. R. J Macromol Sci Polym Rev 2003, 43, 87.
12. Andradi, L. N.; Hellmann, G. P. Polym Eng Sci 1995, 35, 693.
13. Gelfer, M. Y.; Hyun, H. S.; Liu, L.; Benjamin, S. H.; Benjamin, C.; Rafailovich, M.; Mayu, S.; Vladimir, Z. J Polym Sci: Part B 2003, 41, 44.
14. Wang, Y.; Zhang, Q.; Fu, Q. Macromol Rapid Commun 2003, 24, 231.
15. Sinha Ray, S.; Bousmina, M. Macromol Rapid Commun 2005, 26, 450.
16. Sinha Ray, S.; Bousmina, M. Macromol Rapid Commun 2005, 26, 1639.
17. Voulgaris, D.; Petridis, D. Polymer 2002, 43, 2213.
18. Khatua, B. B.; Lee, D. J.; Kim, H. Y.; Kim, J. K. Macromolecules 2004, 37, 2454.
19. Li, Y.; Shimizu, H. Polymer 2004, 45, 7381.
20. Filippone, G.; Dintcheva, N. Tz.; Acierno, D; Mantia, F. P. La. Polymer 2008, 49, 1312.
21. Zou, H.; Ning, N.; Su, R.; Zhang, Q.; Fu, Q. J Appl Polym Sci 2007, 106, 2238.
22. Wu, D.; Zhou, C.; Zhang, M. J Appl Polym Sci 2006, 102, 3628.
23. Kato, M.; Okamoto, H.; Hasegawa, N.; Tsukigase, A.; Usuki, A. Polym Eng Sci 2003, 43, 1312.
24. Gopakumar, T. G.; Lee, J. A.; Kontopoulou, M.; Parent, J. S. Polymer 2002, 43, 5483.
25. Smith, A. P.; Spontak, R. J.; Koch, C. C.; Smith, S. D.; Ade, H. Macromol Mater Eng 2000, 274, 1.
26. Utracki, L. A.; Shi, Z. H. Polym Eng Sci 2004, 32, 1824.
27. Utracki, L. A. Polymer Alloys and Blends: Thermodynamics and Rheology; Hanser: Munich, 1990.
28. Huitric, J.; Mederic, P.; Moan, M.; Jarrin, J. Polymer 1998, 39, 4849.
29. Filippone, G.; Netti, P. A.; Acierno, D. Polymer 2007, 48, 564.
30. Ha, C.-S.; Park, H.-D.; Cho, W.-J. J Appl Polym Sci 2000, 76, 1048.
31. Favis, B. D. Polymer 1994, 35, 1552.
32. Willemse, R. C.; Posthuma De Boer, A.; Van Dam, J.; Gotsis, A. D. Polymer 1999, 40, 827.
33. Willemse, R. C.; Posthuma De Boer, A.; Van Dam, J.; Gotsis, A. D. Polymer 1999, 39, 5879.
34. He, J.; Bu, W.; Zeng, J. Polymer 1997, 38, 6347.
35. Lee, J. K.; Han, C. D. Polymer 2000, 41, 1799.
36. Paul, D. R.; Barlow, J. W. J Macromol Sci Rev Macromol Chem 1980, 18, 109.
37. Utracki, L. A. J Rheol 1991, 35, 1615.
38. Krishnamoorti, R.; Giannelis, E. P. Macromolecules 1997, 30, 4097.
39. Fornes, T. D.; Yoon, P. J.; Keskkula, H.; Paul, D. R. Polymer 2001, 42, 9929.
40. Wildes, G.; Keskkula, H.; Paul, D. R. Polymer 1999, 40, 5609.
41. Hale, W.; Lee, J.-H.; Keskkula, H.; Paul, D. R. Polymer 1999, 40, 3621.